Robust Networked Control Scheme for Distributed Secondary Control of Islanded Microgrids

Qobad Shafiee, *Student Member, IEEE*, Čedomir Stefanović, *Member, IEEE*, Tomislav Dragičević, *Student Member, IEEE*, Petar Popovski, *Senior Member, IEEE*, Juan C. Vasquez, *Member, IEEE*, and Josep M. Guerrero, *Senior Member, IEEE*

***Abstract*—Distributed secondary control (DSC) is a new approach for microgrids (MGs) by which frequency, voltage, and power can be regulated by using only local unit controllers. Such a solution is necessary for anticipated scenarios that have an increased number of distributed generators (DGs) within the MG. Due to the constrained traffic pattern required by the secondary control, it is viable to implement a dedicated local area communication functionality among the local controllers. This paper presents a new wireless-based robust communication algorithm for the DSC of MGs. The algorithm tightly couples the communication and the control functionality, such that the transmission errors are absorbed through an averaging operation performed in each local controller, resulting in a very high reliability. Furthermore, transmissions from each DG are periodic and prescheduled broadcasts, and in this way, contention over the shared wireless medium is avoided. Real-time simulation and experimental results are presented in order to evaluate the feasibility and robustness endowed by the proposed algorithm. The results indicate that the proposed algorithm is very robust with respect to communication impairments, such as packet delays and random packet losses.**

***Index Terms*—Communication systems, distributed control, microgrid (MG), packet delay, packet losses, secondary control.**

I. Introduction

DUE to a considerable growth in the number of renewable energy sources and distributed generators (DGs), microgrids (MGs) have recently attracted significant attention. An MG is defined as a localized cluster of DGs and loads, placed in low-voltage (LV) and medium-voltage (MV) distribution networks, which can autonomously operate in islanded mode or connected to the main grid [1]. These local grids encompass several technology components: power electronics, control, and communication/information technology. The ideas supporting the formation of the MGs are 1) reducing transmission/distribution losses and preventing electrical network congestion by shifting the generation closer to the consumers/loads; 2) enhancing the reliability of the system and gradually reducing the chance for blackouts, as MGs can operate in islanded mode during system disturbances and faults; and 3) provision of ancillary services to the main grid in the grid-connected mode.

However, apart from these obvious benefits of MGs, their introduction into the traditional distribution network raises many new challenges, with one of the most important being frequency and voltage participation in islanded operation mode. This problem has been the focus of many recent works [1]–[8]. To that end, a hierarchical control concept from the traditional power system has been introduced for MGs in [1] and [2]. The first level of this hierarchy is *primary control*, which is strictly local and deals with the inner voltage and current control loops and droop control of the individual DGs in order to adjust the frequency and amplitude according to active and reactive power of the units. When the MG is perturbed by either load variations or connection/disconnection of the units, the primary level is not able to regulate the frequency and voltage of the system. Then, *secondary control* is often employed in order to remove the frequency and voltage deviations in steady state and to achieve global controllability of the MG. Furthermore, the secondary control may share power between units of the MG in cases when primary control is unable to do it [7]. *Tertiary control* is responsible for global optimization of the MG and managing power flow between MGs and the distribution network of the main grid [9]. Usually, the primary and tertiary control levels are decentralized and centralized control levels, respectively, whereas secondary control can be implemented in both centralized and decentralized way [7].

In centralized secondary control (CSC), all DGs measure signals of interest and send them to a common single MG central controller (MGCC), which, in turn, produces appropriate control signals based on the received data and forwards it to the local primary control of the DGs [1], [6]. The exchange of measurements and control signals requires an underlying communication network. Although straightforward to implement, the centralized control strategy has an inherent drawback of the single point of failure, i.e., an MGCC failure terminates the secondary control action for all units [1].

The distributed secondary control (DSC) strategy is a new approach [7], [8] that avoids the use of a single centralized controller for the secondary level of MGs. In this architecture, the primary and secondary controllers are implemented together locally in each DG, where the secondary control should collect the required data from all other units and produce

Manuscript received April 7, 2013; revised September 3, 2013; accepted October 23, 2013. Date of publication December 5, 2013; date of current version May 2, 2014.

Q. Shafiee, T. Dragičević, J. C. Vasquez, and J. M. Guerrero are with the Department of Energy Technology, Aalborg University, 9220 Aalborg, Denmark (e-mail: qsh@et.aau.dk; tdr@et.aau.dk; juq@et.aau.dk; joz@et.aau.dk).

Č. Stefanović and P. Popovski are with the Department of Electronic Systems, Aalborg University, 9220 Aalborg, Denmark (e-mail: cs@es.aau.dk; petarp@es.aau.dk).

Color versions of one or more of the figures in this paper are available online at http://ieeexplore.ieee.org.

Digital Object Identifier 10.1109/TIE.2013.2293711

appropriate control signal for the primary one using an averaging method. Data exchange for DSC can be implemented in several ways, ranging from simple all-to-all transmissions [7] to more involved schemes based on distributed consensus algorithms [10]. The former approach is conceptually simple but does not scale, as the number of required data exchanges quadratically grows with the number of DGs. Distributed consensus relies on a series of local data exchanges among neighboring units to achieve global information dissemination; its use for information dissemination in MGs has been recently proposed in [11] and [12].

In this paper, we present a simple networked control scheme for the DSC of MGs, which exploits the broadcast nature of the wireless medium. The proposed scheme is discrete-time and operates in rounds. In each round, a nontransmitting DG attempts to receive the broadcast packet, updates its local record on the averages of the parameters, and derives the local control signal accordingly. The broadcasts are performed by units in a token ring manner, representing a current record of the respective unit averages. Even though the proposed scheme is conceptually similar to the schemes that exploit distributed consensus [11], [12], the major difference is that the communications and control layers are not separated, but the scheme exploits their inherent feedback loop. Specifically, rather than waiting for a series of local data exchanges to converge to the global average at every DG, in the proposed approach, the control signal is locally updated after each data exchange, enforcing the MG toward the desired operation point. We show that the proposed scheme enhances reliability of DSC, making it robust against delays and packet losses in the wide range of wireless link conditions. In addition, the proposed scheme is designed not only for the regulation of frequency and voltage but also for power sharing among the units, maintaining the power-sharing feature of the primary droop controller.

This paper is organized as follows: Section II provides an overview of the background and related work. The DSC of islanded MGs is presented in Section III. In Section IV, the proposed communication algorithm for DSC is elaborated. Section V provides simulation results of an islanded MG with four units, evaluating the proposed algorithm for DSC. An experimental validation of the proposed solution in an islanded MG with two units is presented in Section VI. Section VII concludes this paper and outlines future research directions.

II. Background and Related Work

When a traditional feedback control system is closed via a communication network, the control system is classified as a networked control system (NCS) [13]. Fig. 1 illustrates the general structure of an NCS. The communication network is the backbone of the NCS, and its reliability, security, ease of use, and availability are the main issues that affect the actual choice of the communication technology to be employed [13]. Several communication technologies have been introduced for NCSs, both wired and wireless [13]. The advantages of the wireless NCSs over wired solutions are flexibility, expandability, and mobility support. On the other hand, wireless NCSs exhibit a lower degree of reliability, which can have a destructive effect

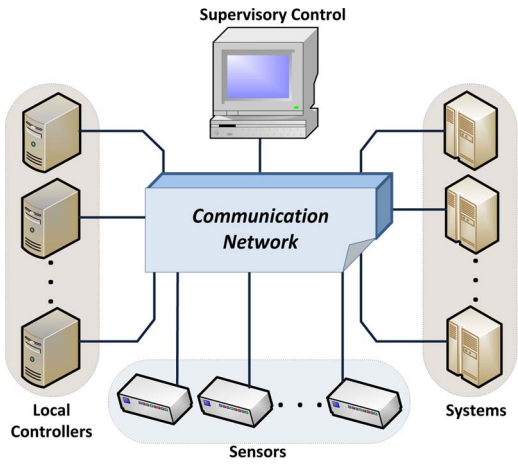

Fig. 1. General structure of NCSs.

on the system performance. Communication impairments, such as packet delays and losses, may compromise the stability of the system, such that their modeling and analysis reveals important effects on NCSs [13], [14].

Use of NCSs for MGs has been recently reported in [3] and [15]–[17]. The work in [3] investigates the technical aspects of providing frequency control reserves (FCRs) and the potential economic profitability of participating in FCR markets for both decentralized and centralized coordination approaches for multiple MGs. In [15], a pseudo-decentralized control strategy has been presented for distributed generation networks, which operate in a distributed manner. Master–slave control using a networked control strategy for the parallel operation of inverters has been introduced in [16], achieving superior load-sharing accuracy compared with the conventional droop scheme. Finally, [17] presents an impact analysis of communications in frequency and active power control in hierarchic multi-MG structures, considering both packet delays and losses.

From the NCS perspective, DSC requires that every DG obtains the global average of the parameters of interest, i.e., frequency, voltage, and active and/or reactive power, in order to derive the local control signals. The provision of global averages is the task of underlying communication infrastructure, which may be achieved in a number of ways. A scalable and robust approach is to employ distributed averaging algorithms [10], where a series of local exchanges among neighboring units ultimately yields the same global average at every DG. The convergence of distributed averaging relies on the general theory of Markov chains with a doubly stochastic transition matrix. The convergence rate depends on network size, topology, and transition matrix design; the number of iterations (i.e., number of local data exchanges) required for local estimates to closely approach the actual value of the global average may be quite large in practice, even for rather simple networks [10], [18].

The utility of distributed consensus algorithms for MGs was considered in [11]. Based on these principles, the same authors investigated the enhancements of droop control by information exchange concerning active and reactive power in MG. In the related analysis, the communication delay was assumed to be negligible, and the stability of the control algorithm

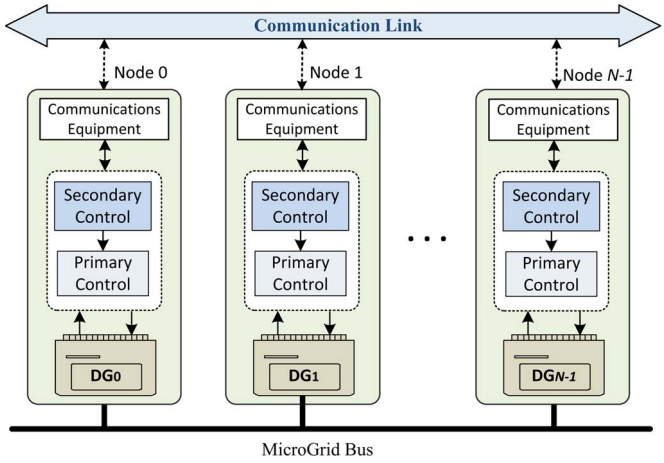

Fig. 2. General architecture of DSC for islanded MGs.

was considered in the presence of (data) packet losses. The problem of packet losses for networked control of DGs was also addressed in [12], where an iterative distributed averaging algorithm robust to packet losses was derived and applied for the problem of coordinating DGs for the reactive power support for voltage control.

The solution proposed in this paper also falls into the category of the distributed averaging algorithms; more specifically, it can be categorized as a broadcast gossip algorithm [21]. However, the novelty of our approach is that it tightly couples the communication and control layers in DSC, rather than considering them separately. After each iteration, both the local estimates of the global averages of interest and the corresponding local control signals are updated. That is, the control layer does not stop its operation and waits for the communication layer to provide local estimates that are sufficiently close to each other, but it operates in parallel, based on their current values. As these estimates start to converge, the control layer further drives operation of every DG in the "direction" of the global average, boosting the algorithm convergence rate. In this sense, the proposed scheme represents a tightly coupled NCS. The proposed scheme is demonstrated for MGs that have all DGs within the communication range of each other, which is typically the case in practice for LV MGs. However, the convergence of broadcast-based gossiping [21] extends the relevance of the proposed solution for connected multihop networks.

III. DSC of Islanded MGs

A distributed control strategy is an approach in which none of the controllers are centralized, but distributed throughout the system so that each unit is independently controlled and the entire system of controllers is connected by a communication network. Fig. 2 illustrates the implementation of the distributed control strategy. As shown, secondary control is locally embedded in each DG unit, similar to primary control; however, the local secondary control requires an underlying communication network to operate properly. The combined communication–control algorithm, presented in Section IV, is used to exchange and update averages of the parameters of interest to secondary controllers. In turn, the local secondary controllers operate on these parameters, regulating the frequency and voltage of the system and sharing power between the units.

Conventional CSC is only responsible for restoring frequency and voltage inside the whole MG using common measurements of the system [1], [6]. However, DSC using the proposed communication algorithm is able to not only control frequency and voltage but also share power between units in the MG. We continue by elaborating the used DSC algorithm in detail; henceforth, we assume that the MG consists of N DG units, denoted as $DG_0, DG_1, \ldots, DG_{N-1}$.

A. Frequency and Voltage Control

Load frequency control as a major function of automatic generation control (AGC) systems is the central secondary control for frequency regulation in large power systems, as frequency is a control variable that provides information related to the consumption/generation balance of the grid. Taking the idea from large power systems, a CSC is implemented in the MG in order to regulate the frequency of the whole system. However, in the distributed strategy, each DG has its own local secondary control to regulate the frequency. In this sense, each unit measures its frequency at each sampling instant, averaging the received information from other units and then broadcasting its average version $(\bar{f}_{\mathrm{MG}})$ to the other units through the communication network. The averaged data are compared with the nominal frequency of MG (f^*_{MG}) and sent to the secondary controller of DG_i to restore the frequency as follows:

$$\delta f_s = k_{pf}\left(f^*_{\mathrm{MG}} - \bar{f}_{\mathrm{MG}}\right) + k_{if}\int\left(f^*_{\mathrm{MG}} - \bar{f}_{\mathrm{MG}}\right)dt \quad (1)$$

where k_{pf} and k_{if} are the control parameters of the PI compensator of unit i, and δf_s is the secondary control signal sent to the primary control level in order to remove the frequency deviations.

Since the Q-V droop control is not able to regulate the voltage in the MG, a controller similar to the one controlling frequency can be implemented in the secondary control level for voltage restoration [1], [6]. In this secondary voltage control strategy, after calculating the average value of voltage $\bar{E}_{\mathrm{MG}}$ that is based on the information exchanged over the communication network, every local secondary controller measures the voltage error and compares it with the voltage reference of MG, i.e., E^*_{MG}. In the next step, the local secondary controller sends control signal δE_s to the primary level of control as a set point to compensate for the voltage deviation. The voltage restoration control loop of DG_i can be expressed as follows:

$$\delta E_s = k_{pE}\left(E^*_{\mathrm{MG}} - \bar{E}_{\mathrm{MG}}\right) + k_{iE}\int\left(E^*_{\mathrm{MG}} - \bar{E}_{\mathrm{MG}}\right)dt \quad (2)$$

with k_{pE} and k_{iE} being the PI controller parameters of the voltage secondary control. The above secondary control strategy can be also extended to more-resistive-line MGs that are using P-V and Q-f droops in the primary control, to regulate frequency and voltage. Consequently, secondary control is applicable to the all-resistive/inductive (R/X) nature of the power lines, as opposed to primary control.

B. Power Sharing

In a low R/X MG, reactive power is difficult to be precisely shared between units using Q-V droop control, since voltage is not common in the whole system as opposed to frequency. Furthermore, the impedance between the DG units and the point of common coupling is not necessarily the same; a similar effect occurs when trying to equalize active power of units using P-V in high-resistive-line MGs.

An alternative solution is to implement a distributed average power sharing in the secondary loop, where the averaging is performed through the communication network. This way, all units obtain the same reference, and power sharing is independently achieved from voltage sensing mismatches or line impedance values in the MG. The distributed averaged power sharing by the secondary control of DG_i can be expressed as follows:

$$\delta Q_s = k_{pQ}(Q_i - \bar{Q}_{\mathrm{MG}}) + k_{iQ}\int (Q_i - \bar{Q}_{\mathrm{MG}})dt \qquad (3)$$

where k_{pQ} and k_{iQ} are the PI controller parameters, Q_i is the locally calculated reactive power (which can be active power in the case of high-resistive-line MGs), $\bar{Q}_{\mathrm{MG}}$ is the average power obtained through the communication network, and δQ_s is the control signal produced by the secondary control in each sample instant and afterward sent to the primary loop. Normally, bandwidth must be decreased with an increase in the control level of MG. For the proposed control scheme, the bandwidth of the power-sharing loop must be considered lower than droop control but greater than the bandwidth of the frequency and voltage secondary control loop.

It is worth noting that the interaction of active power sharing and frequency control in the proposed scheme shows similarity to the traditional AGC where both frequency regulation and power flow control are simultaneously achieved. A detailed block diagram of the DSC strategy for an individual high-inductive-line DG (DG_i) in an islanded power-electronic-based MG is shown in Fig. 3; the figure shows a general scheme of the primary control as well. Antiwindup saturation blocks are implemented for every PI controller of secondary control in order to protect the units in case of extreme contingencies. (Interested readers can find more detail about primary control in [6].)

C. Modeling and Small-Signal Stability Analysis

In order to analyze the stability of the system and to adjust the parameters of DSC, a small-signal model has been developed. Fig. 4 shows the equivalent circuit of n inverters connected to an ac bus. It is assumed that the output impedance of the inverters is mainly inductive $(\theta = 90^\circ)$. In this situation, the active power and reactive power injected into the bus by every inverter are expressed as the following well-known equations [19], [20]:

$$P_i = \frac{E_i V \sin\phi_i}{X_i} \qquad (4)$$

$$Q_i = \frac{E_i V \cos\phi_i - V^2}{X_i} \qquad (5)$$

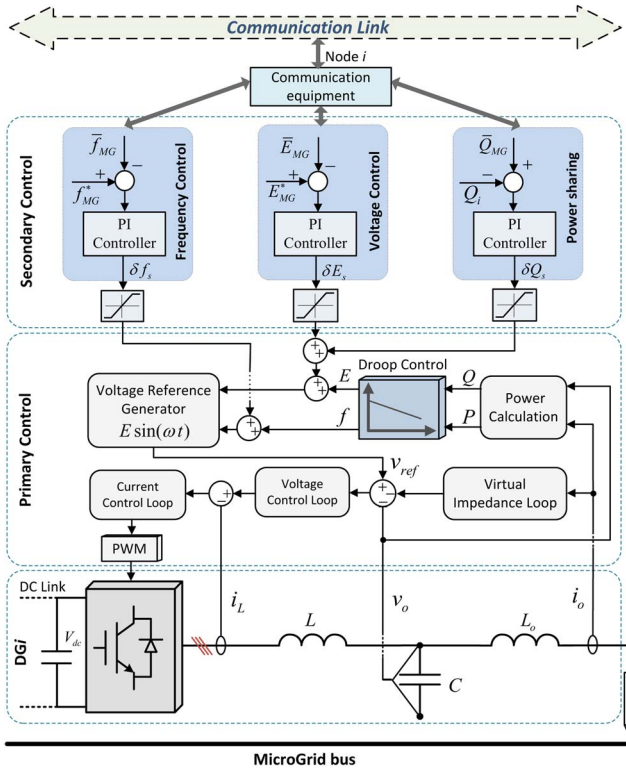

Fig. 3. Details of the proposed DSC for an individual DG in an islanded MG.

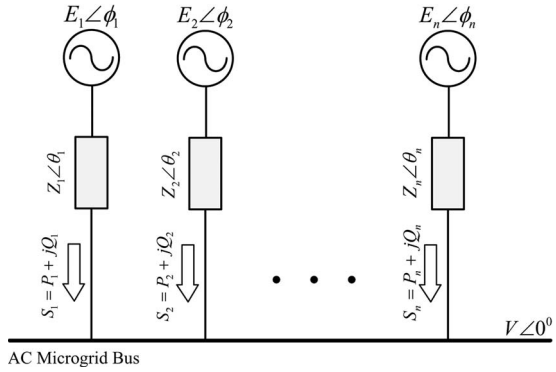

Fig. 4. Equivalent circuit of n parallel inverters connected to an ac bus.

where E_i and V are the amplitudes of the ith inverter output voltage and the common bus voltage, ϕ_i is the power angle of the inverter, and X_i is the magnitude of the output reactance for the ith inverter. From the given equations, it can be seen that if the phase difference between E_i and V is small enough, the active power is strongly influenced by power angle ϕ_i, and the reactive power flow depends on the voltage amplitude difference. Consequently, the frequency and the amplitude of the inverter output voltage can be expressed by the well-known droops as [19]

$$\omega_i = \omega^* - k_p P_i \qquad (6)$$

$$E_i = E^* - k_q Q_i \qquad (7)$$

where ω^* and E^* are the output voltage frequency and amplitude references, and k_p and k_q are the droop frequency and amplitude coefficients. To realize the droop functions, it is

necessary to employ low-pass filters (LPFs) in order to calculate the active and reactive power from the instantaneous power. The bandwidth of the LPF must be smaller than that for the closed-loop inverter. As aforementioned, the outputs of secondary control obtained through (1)–(3) are added to the droops to shift the droop lines in order to restore the frequency and voltage of the system and to share the power between the units. It is worth noting that a phase-locked loop (PLL) is used to extract the frequency of the units inside the system. Therefore, (6) and (7) are updated as

$$\omega_i = \omega^* - k_p P_i + \delta\omega_s \tag{8}$$
$$E_i = E^* - k_q Q_i + \delta E_s + \delta Q_s. \tag{9}$$

To study the dynamics of the system, a small-signal model is obtained by linearizing (4), (5), (8), and (9) at operating points P_{ie}, Q_{ie}, E_{ie}, V_e, and ϕ_{ie} as follows [20]:

$$\Delta\omega_i(s) = \Delta\omega^*(s) - k_p\Delta P_i(s) + \Delta\omega_s(s) \tag{10}$$
$$\Delta E_i(s) = \Delta E^*(s) - k_q\Delta Q_i(s) + \Delta E_s(s) + \Delta Q_s(s) \tag{11}$$
$$\Delta\phi_i = \int \Delta\omega_i dt \tag{12}$$
$$\Delta P_i(s) = G\Delta\phi_i(s) \tag{13}$$
$$\Delta Q_i(s) = H\Delta E_i(s) + F\Delta V(s) \tag{14}$$

where

$$G = \frac{E_{ie}V_e\cos\phi_{ie}}{X_i}, \quad H = \frac{2E_{ie} - V_e\cos\phi_{ie}}{X_i}$$
$$F = -\frac{E_{ie}\cos\phi_{ie}}{X_i}.$$

Fig. 5 shows block diagrams representing the small-signal model for both frequency and voltage control of the system as well as reactive power sharing. The block diagrams include the plant model, the droop control model, and the decentralized secondary control model. As can be observed, an LPF with a cutting frequency of 0.5 Hz has been considered for power calculation $(G_{\mathrm{LPF}}(s))$, and a simplified phase-locked loop (PLL) first-order transfer function $(G_{\mathrm{PLL}}(s))$ is used to extract the frequency of the units.

The dynamics of the system around the operating point may be expressed in state-space form as follows:

$$\dot{x}(t) = Ax(t) \tag{15}$$

where for the frequency control model [see Fig. 5(a)], x is $[x_1\ x_2\ x_3\ x_4]^T$, and A is

$$A = \begin{bmatrix} -\frac{1}{\tau_p} & 0 & 0 & G \\ -\frac{k_p}{\tau_p} & -\frac{1+k_{pf}}{\tau} & 1 & 0 \\ 0 & -\frac{k_{if}}{\tau} & 0 & 0 \\ -\frac{k_p}{\tau_p} & -\frac{k_{pf}}{\tau} & 1 & 0 \end{bmatrix}. \tag{16}$$

The state variables x_1, x_2, x_3, and x_4 are assigned to the output of LPF, PLL, PI controller, and the integral term of the power angle, respectively. For voltage control [see Fig. 5(b)], x represents $[x_1\ x_2]^T$, where state variables x_1 and x_2 are chosen

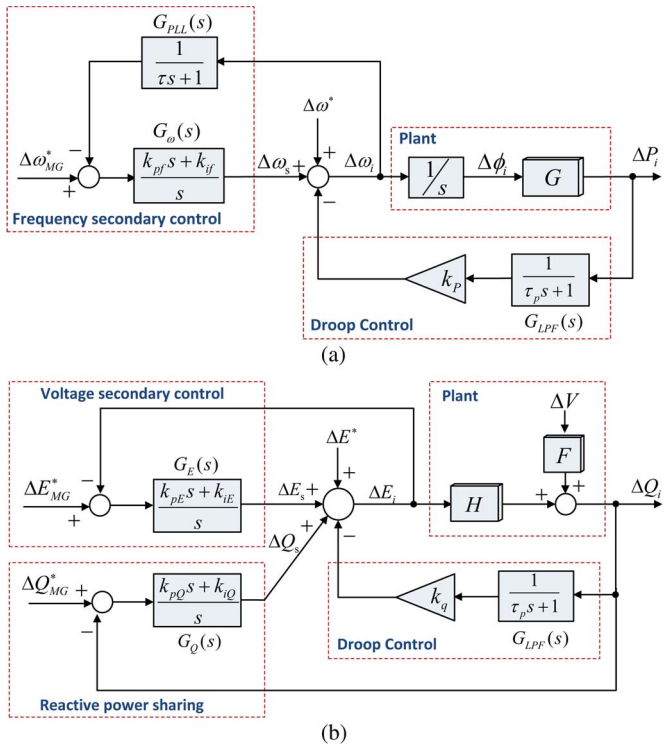

Fig. 5. Small-signal representation of frequency and voltage control and reactive power sharing. (a) Frequency control model. (b) Voltage control and reactive power-sharing model.

as the state variable of LPF and PI controller, respectively, and A is presented as

$$A = \begin{bmatrix} -\frac{1+k_{pE}+k_qH}{\tau_p(1+k_{pE})} & \frac{H}{1+k_{pE}} \\ \frac{k_qk_{iE}}{\tau_p(1+k_{pE})} & -\frac{k_{iE}}{1+k_{pE}} \end{bmatrix}. \tag{17}$$

The eigenvalues of matrix A can be used to study the stability of the system around the state of equilibrium. For the calculation of plant parameters (G, H, and F), we can choose $E_{ie} = 1$ per unit, $V_e = 1$ per unit, and $\phi_{ie} = 0$, since the amplitude and phase adjustments made by each unit are very small compared with the nominal value of voltages, and the phases are always initially in synchronization with respect to the reference voltage. Moreover, we assume $X_i = 0.001$ per unit. Other needed parameters can be found in Table I.

Fig. 6 shows the trajectory of the low-frequency eigenvalues of both the frequency and voltage models as a function of the secondary control parameters. This figure shows that as the proportional terms of PI controllers are increased, the eigenvalues of the system move toward an unstable region, making the system more oscillatory and eventually leading to instability. However, the integral term parameter has no significant effect on the dynamics of the system. Similar analysis can be performed for the other parameters of the presented model.

IV. Proposed Broadcast Algorithm

As already noted, the proposed communication solution falls into the category of broadcast gossip algorithms for consensus [21]; we provide their brief overview in the Appendix. In this paper, we treat the simplest case in which we assume that

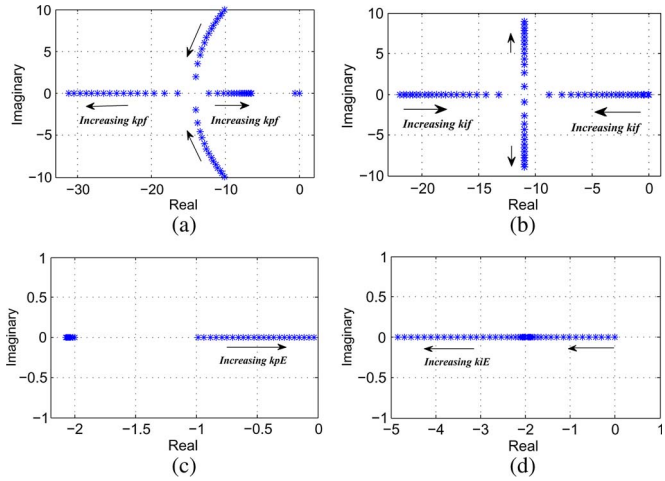

Fig. 6. Trace of low-frequency eigenvalues as a function of secondary control parameters. (a) and (b) Frequency control. (c) and (d) Voltage control.

all units are in the communication range of each other; the motivation is to demonstrate the potential of the proposed NCS solution and avoid the complexities coupled with a more general approach. However, we note that results presented in [21] grant applicability of the proposed NCS solution for multihop networks as well.

We assume that communication occurs in discrete periodic time instants and that all units are assumed to be synchronized to that periodic communication structure. Note that this synchronization requires packet-level precision, not symbol-level precision, which makes it very practical. At each time instant k, each unit measures the parameters of interest, i.e., frequency, voltage, and power. In the following text, we present the algorithm for the distributed averaging of a general parameter x, which can stand for frequency, voltage, or power.

The measurement of x made by DG_i at the kth time instant is denoted by $x_i(k)$. The current local estimate of the global average a of parameter x that is computed by DG_i at instant k is denoted by $a_i(k)$. At the kth time instant, the unit that is allowed to broadcast is DG_j, where $j = k \bmod N$. Such a rule implements a token-ring-like broadcasting scheme among the N DGs.[1] The signal broadcasted at the kth time instant can be written as

$$b(k) = a_j(k), \qquad \text{where } j = k \bmod N. \tag{18}$$

The local estimates $\{a_i(k)\}$ of all DGs, including the broadcasting one, are updated as follows:

$$a_i(k) = \beta_i x_i(k) + (1-\beta_i) b_i(k), \qquad i = 0, 1, \ldots, N-1 \tag{19}$$

where $b_i(k)$ is the local record of the received broadcast signal, i.e.,

$$b_i(k) = b(l_i), \qquad l_i < k \tag{20}$$

and l_i denotes the time instant at which the last successful broadcast has been received by agent DG_i. In case when there are no packet losses $b_i(k) = b(k-1)$, $i = 0, 1, \ldots, N-1$. Finally, β_i is suitably chosen constant that determines the weight

[1]More information about the token ring can be found in [22].

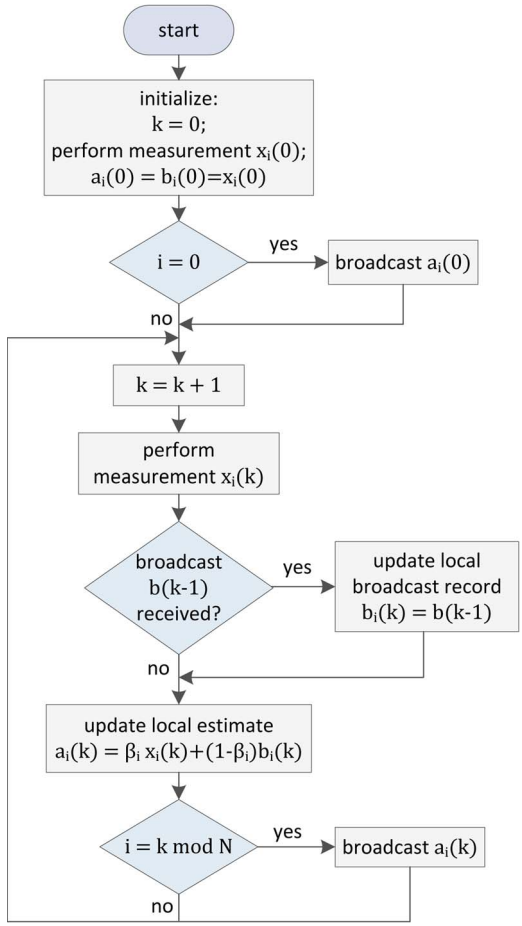

Fig. 7. Flowchart of the proposed algorithm, as executed in unit DG_i.

of the measurement made by D_i when computing the estimate; a straightforward choice is to set $\beta_i = 1/N$, $i = 0, 1, \ldots, N-1$.

Fig. 7 shows the flowchart of the algorithm from the perspective of a DG unit. The first step is initialization, when the local records of the broadcast and average are set to initial measurement, followed by the initial broadcast performed by DG_0. In the next steps, DG units execute the command loop, which consists in measuring the parameter, receiving the updating broadcast signal, updating the average, and broadcasting the local estimate every Nth instant.

The algorithm can be interpreted as if the units use broadcasts to exchange the local estimates of the global average. As these estimates contain the locally measured values, the broadcasts actually exchange the information necessary for the computation of the global average. As time progress, the "mixing" of the local measurements in every agent becomes more effective, and the units start converging toward the same global average value. Specifically, in [21] and [24], it was shown that the mean square error (MSE) between the local and the global average is strictly a decreasing function of time, i.e., after each message exchange and computation of the update, the MSE decreases.[2] On the other hand, the locally executed DSC algorithm operates on the local estimates, such that control signals shift the local

[2]More details on the convergence rate of broadcast-based gossip for consensus are given in the Appendix.

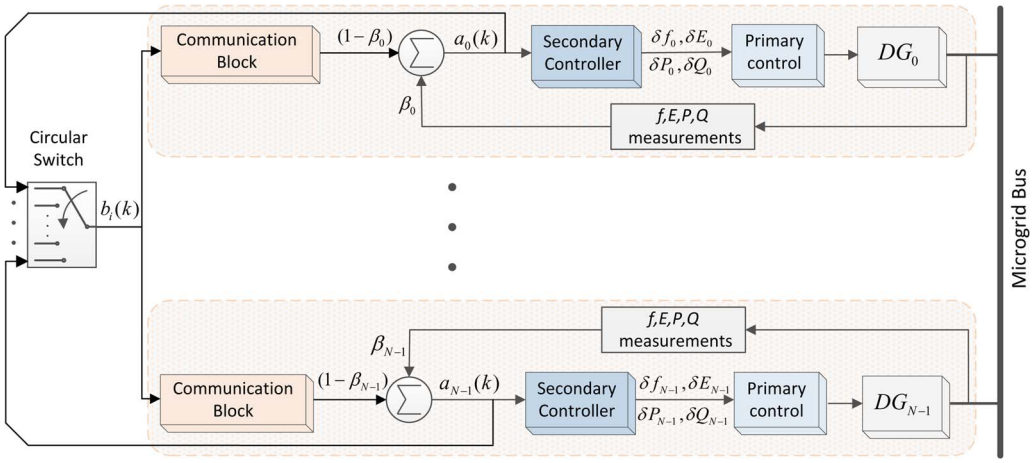

Fig. 8. Implementation of the proposed algorithm on DSC of an islanded MG.

parameter $x_i(k)$ toward the computed local estimate $a_i(k)$ of the global average a, $i = 0, 1, \ldots, N$; that is, the MSE is further decreased by the operation of the control algorithm executed after each broadcast, thus accelerating the convergence toward the desired MG operation.

We note that a rigorous analysis of the convergence rate of the whole NSC solution would have to include an analytical model of the primary and secondary control, as well as their interdependence relations with the distributed gossip algorithm, representing a rather complex problem in its own right that is outside the scope of this paper.

The actual rate of information exchange, i.e., how often broadcasts are performed, primarily depends on the characteristics of the employed communication technology. In a typical MG setup, the wireless propagation delays can be neglected, and the dominant component of the communication delay is the processing performed by the protocol stack.[3] This consists of reception of the broadcast packet, update of the local estimate, and transmission of the update. As an example, we have performed an experimental study that showed that the minimum expected delay in IEEE 802.11 (WiFi) from the moment of packet reception until completion of broadcasting is of the order of 10 ms, implying that the update information in the network can be exchanged roughly at the rate of 100 Hz, i.e., 100 times in a second. Nevertheless, this rate is rather adequate for DSC, since, in contrast to primary control, the secondary and tertiary controllers in MGs typically operate with low sampling rates [1].

The proposed scheme requires synchronization and transmission scheduling among DGs, both of which can be also established using broadcast gossip algorithms [23] and which could be executed in the initial setup phase of the network.[4] Moreover, distributed synchronization and scheduling should be reestablished whenever the network topology changes and the corresponding communication exchanges triggered by detection of such events; however, the details of a corresponding full-blown detailed protocol solution are out of the scope of this paper.

[3]Note that we assess a steady-state operation, when the scheduling has been already established and there are no collisions among agents' transmissions.

[4]Another highly reliable approach for synchronization is to equip all DGs with GPS receivers that supply a very accurate time reference.

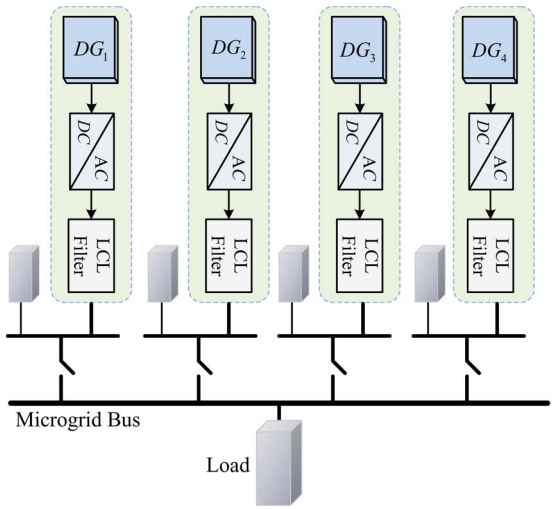

Fig. 9. Simulation case study: an islanded MG with four units.

We conclude this section by displaying a block diagram that represents the proposed NCS, as given in Fig. 8. As shown, DGs are interconnected through the power and communication network, and each DG implements the same primary control, as well as the combined communication/secondary control. We note that the circular switch only models the operation of the scheduling, which is actually implemented in a distributed way across the network nodes. In Sections V and VI, we demonstrate the potential of the proposed networked control solution in simulation and laboratory setups, respectively.

V. Hardware-in-the-Loop Simulation Results

In order to evaluate the effectiveness of the proposed algorithm for DSC, an islanded low R/X MG consisting of four DGs is considered as a case study, as shown in Fig. 9. All units in the system have the same power rate of 2.2 kW, and each one is supporting a local load; units 1–4 feed 200-, 400-, 200-, and 400-Ω resistive loads, respectively. The electrical part of the system has been implemented in MATLAB SimPower Systems and the control part in MATLAB Simulink. The dSPACE 1103 is a real-time platform used as an interface between the electrical part and the control part to produce a power hardware-in-the loop (PHIL) simulation. The proposed communication

TABLE I
ELECTRICAL SETUP AND CONTROL SYSTEM PARAMETERS

Parameter	Symbol	Value
Electrical parameters		
Nominal voltage	E	311 V
Nominal frequency	$f^*/2\pi$	50 Hz
DC Voltage	V_{dc}	650 V
Output inductance	L_o	1.8 mH
Filter inductance	L	1.8 mH
Filter capacitance	L	25 μF
Load	$R_L(t)$	200,400 Ω
dSPACE sampling frequency	f_s	10 kHz
Droop Control		
Proportional frequency droop	k_p	0.0008 W/rd·s
Proportional amplitude droop	k_q	0.16 VAr/V
DSC		
Frequency proportional term	k_pf	0.01
Frequency Integral term	k_if	4 s^{-1}
Voltage proportional term	k_pE	0.01
Voltage Integral term	k_iE	0.6 s^{-1}
Reactive power proportional term	k_pQ	0.00001 VAr/V
Reactive power integral term	k_iQ	0.3 VAr/Vs
PLL time constant	τ	0.05 s

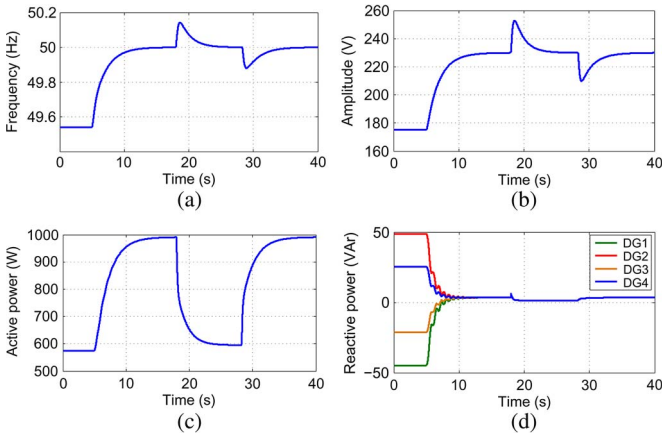

Fig. 10. Performance of DSC with the proposed algorithm for an islanded MG with four units. (a) Frequency restoration. (b) Voltage restoration. (c) Active power sharing. (d) Reactive power sharing.

algorithm has been implemented in MATLAB Stateflow, which provides a graphical interface for modeling sequential decision and temporal logic flowcharts and is fully compatible with dSPACE. Communication delay and packet losses have been modeled in MATLAB Stateflow as well. The electrical setup and control system parameters are detailed in Table I.

All the simulation results have been extracted from dSPACE control desk but plotted using MATLAB to have better quality. Fig. 10 shows simulation results for different scenarios evaluating the performance of the proposed DSC. Fig. 10(a) shows restoration of the frequency to its nominal value. Specifically, during the first 5 s of operation, where the MG is under only the primary P-f droop controller, a steady-state frequency deviation from the nominal value exists. In order to remove the deviation, the proposed DSC is implemented at $t = 5$ s, and as can be observed, the system frequency is successfully regulated. The performance of the proposed DSC in the presence of frequent load changes is evaluated in the latter half of the simulation, where a 200-Ω load was connected for a short time at $t = 17$ s

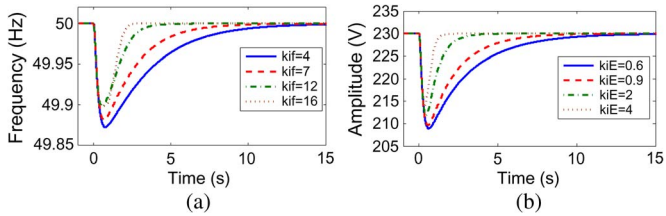

Fig. 11. Verifying the sensitivity of the proposed DSC to the PI parameters. (a) Frequency response. (b) Voltage response.

and then disconnected at $t = 27$ s. As can be observed, the DSC using the proposed algorithm is able to regulate the MG frequency despite these rapid load variations. Fig. 10(c) shows the corresponding active power injections of four units in the same scenarios, illustrating that the primary P-f droop method is sufficient to share the active power accurately between the units and that the DSC preserves the power-sharing properties established by the primary controller. Since the load is resistive, a considerable increase in active power is observed in the first half of the simulation when the DSC tries to remove the steady-state frequency deviations. Frequent active power changes in the second half of the simulation is due to the aforementioned frequent load switches. It is worth mentioning that for units with different power rates, the DSC may consider different coefficients for its output signals.

Fig. 10(b) depicts how the proposed DSC regulates voltage amplitude inside the MG. Similar to P-f droop control frequency deviations, Q-V droop control also produces substantial voltage deviations, as seen in the first 5 s of simulation. When the DSC is enabled at $t = 5$ s, the voltage is well restored, removing the static deviation produced by droop control. The figure illustrates that the DSC also has a good performance when rejecting voltage disturbances caused by load variations. Fig. 10(d) represents the effectiveness of the proposed secondary control strategy for sharing reactive power among all four units. It can be observed that the primary droop control alone is not able to equalize the reactive power of DGs in the MG. After implementing the DSC, reactive power is properly shared between DGs, even in the presence of load variations.

It is worth noting that the speed of secondary control can be enhanced by increasing the parameters of PI controllers, as shown in Fig. 11. However, the speed increase is limited both by the communication network and the bandwidth of the primary control.

In order to verify the sensitivity of the proposed control system to the controller parameters, some simulation results are presented in Fig. 11. This figure shows the frequency and voltage restoration process for different PI parameters (here integral term parameters). The graphs have been extracted when DSC is active, and a load is suddenly added at $t = 0$.

A. *Effects of Packet Delay*

So far, we have assumed that information exchanged via broadcasts represents the most recent state of the DGs. Here, we relax this condition and examine the effects of information delay, which comprises delay due to measurement, processing, transmission, and reception of data. Specifically, the performance of the DSC was investigated for three different delays:

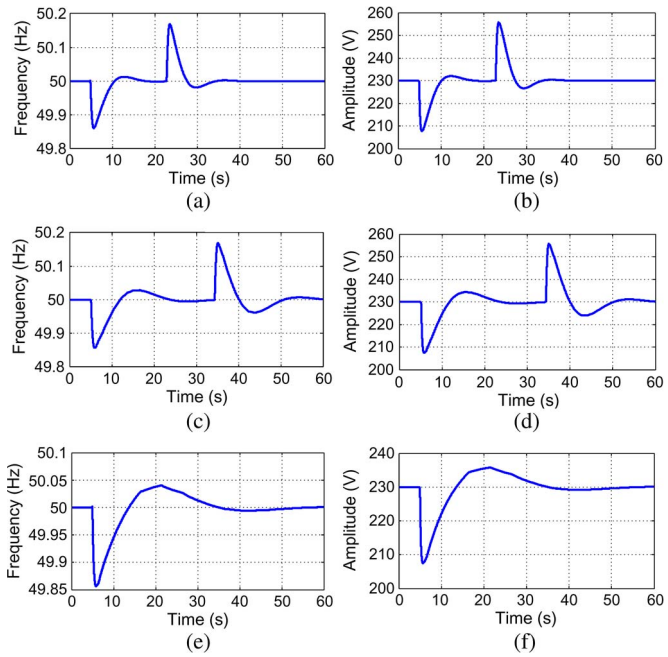

Fig. 12. Evaluation of the proposed DSC in regulating frequency and voltage of the MG considering packet delay. (a) 0.5-s time delay. (b) 0.5-s time delay. (c) 2-s time delay. (d) 2-s time delay. (e) 10-s time delay. (f) 10-s time delay.

0.5, 2, and 10 s. A variable time delay with a standard deviation of 0.5 s was added to the constant delays for all cases. For the sake of simplicity, only frequency and voltage responses are represented.

Fig. 12 illustrates how delay affects the system output, when the DSC tries to remove frequency and voltage deviations caused by frequent load variations. Fig. 12(a) and (b) depicts the frequency and voltage responses of the system to the frequent load switching when the interval duration is set to 0.5 s. In the first half of the simulation, a 200-Ω load is connected to the MG and, in the second half, disconnected again. The same procedure is repeated when the delay is set to 2 s, and the results are plotted in Fig. 12(c) and (d). As can be observed, the proposed scheme exhibits an acceptable response with small overshoots. The last row in Fig. 12 shows robustness of the proposed method, as the MG system is still stable when the delay is 10 s—the DSC slowly but successfully regulates frequency and voltage deviations caused by load variations. We note that when time delay is larger, settling time is bigger compared with the previous cases; thus, only one load change has been shown in 60 s.

B. *Effect of Packet Losses*

To evaluate the impact of erroneously received or lost broadcast packets on the performance of the proposed scheme, we have applied a packet loss probability of 95%. This is exceptionally high and, practically, at the edge of making the links inexistent. To produce the probability of 0 or 1 for the modeling of packet losses, the Bernoulli random process has been used. MATLAB Stateflow has been programmed so that if the input of the Bernoulli random process is 1, then the received broadcast value is used; otherwise, DSC uses the last broadcast value until the new packet arrives. The general convergence of the proposed broadcast gossip algorithm with packet losses is shown in [24].

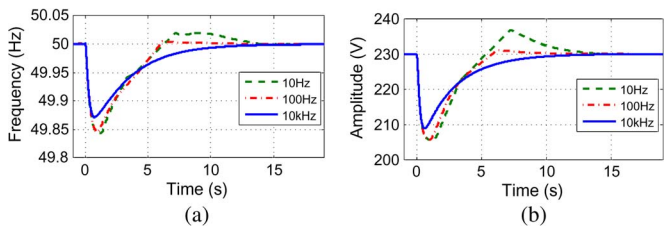

Fig. 13. Impact of packet loss on the performance of the proposed DSC considering different sampling rates. (a) Frequency restoration. (b) Voltage restoration.

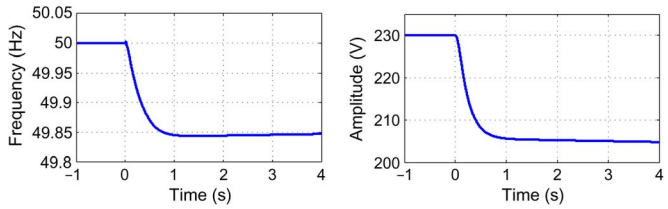

Fig. 14. Frequency and voltage responses in the presence of communication link failure.

Fig. 13 illustrates the effect of 95% packet losses over the frequency and voltage responses of the system when a 200-Ω load is suddenly connected to the MG load bus. Obviously, the lower the sampling rate of the communication algorithm, the more pronounced are the effects of packet losses on the system performance. Nevertheless, it can be observed that the proposed NSC scheme is robust against high probability of packet losses, as voltage and frequency of the MG are properly regulated. The reason for this is that, due to the broadcast nature of the communication algorithm, the chances of a packet getting through to at least one neighbor are significantly higher than the chances of this happening on a single link. We also note that lower values of packet loss probability had virtually no effect on the performance of the proposed algorithm in the examined setup.

Fig. 14 demonstrates what happens if the communication links completely fail (100% packet loss). Obviously, after a load is connected at $t = 0$, the DSC cannot perform the frequency and voltage restoration, as it operates only on local measurements. This implies that communications are indeed necessary for proper DSC operation.

VI. Laboratory-Scale Experimental Results

An islanded power-electronic-based MG consisting of two units was built and tested in the laboratory as a case study in order to evaluate the performance of the proposed algorithm experimentally. The scheme of the experimental setup of an islanded MG system is shown in Fig. 15, in which two Danfoss 2.2-kW voltage source inverters operating in parallel at 10 kHz with LCL output filters supply power to a diode rectifier loaded by a 200-Ω resistor. The primary and secondary control strategies were implemented in MATLAB Simulink and dSPACE 1103, which is a real-time platform used as an interface between the electrical part and the control part. The proposed algorithm

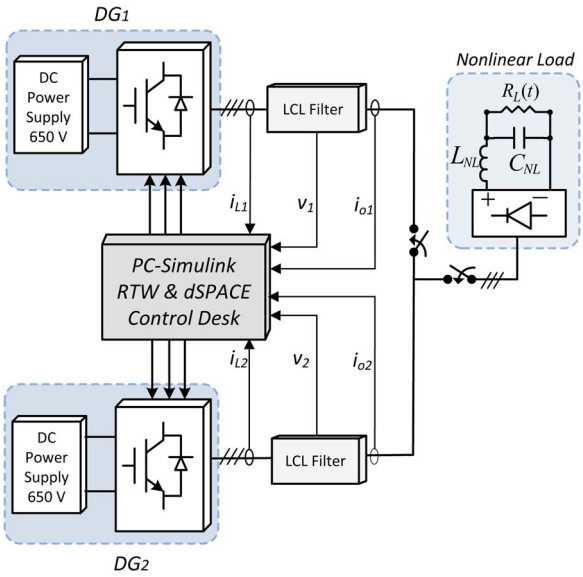

Fig. 15. Experimental setup of an islanded MG with two units.

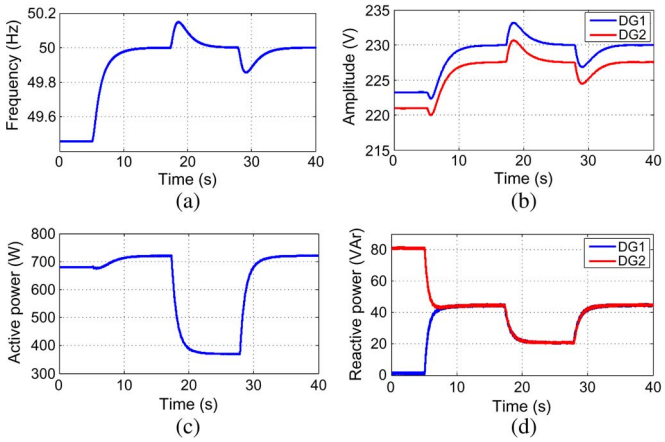

Fig. 16. Experimental validation of the proposed algorithm for DSC of an islanded MG with two units. (a) Frequency restoration. (b) Voltage restoration. (c) Active power sharing. (d) Reactive power sharing.

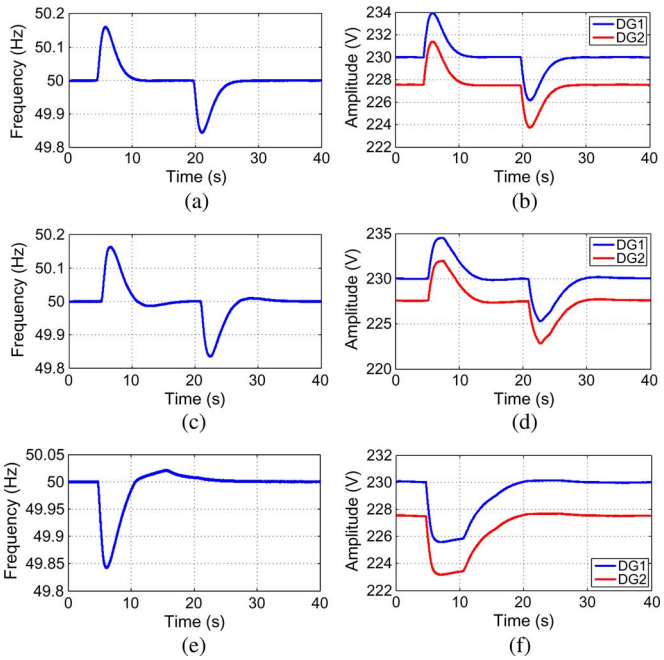

Fig. 17. Experimental evaluation of the proposed DSC in regulating frequency and voltage of the MG considering packet delay. (a) 0.5-s time delay. (b) 0.5-s time delay. (c) 2-s time delay. (d) 2-s time delay. (e) 20-s time delay. (f) 20-s time delay.

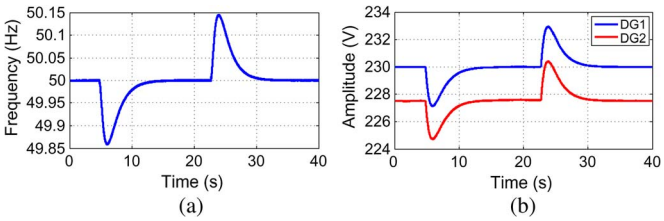

Fig. 18. Evaluation of the proposed DSC in regulating frequency and voltage of the MG considering packet losses. (a) Frequency restoration. (b) Voltage restoration.

was modeled in MATLAB Stateflow. The electrical setup and control system parameters are the same as the simulation part listed in Table I.

Several experimental tests were carried out to validate the effectiveness of the proposed scheme. Similar to the simulation results, the experimental results have been extracted from dSPACE control desk but plotted using MATLAB. Fig. 16 represents the dynamic response of the MG system examined for three different scenarios similar to those performed in Section V. During the first one, only primary control is running, and the DSC is not enabled. As shown in Fig. 16, not only P-f and Q-V droops deviate frequency and voltage of the MG, but also poor reactive power sharing between units is exhibited. Nevertheless, active power is shared properly between units using the P-f droop since the frequency is the same in the whole MG. When the proposed DSC is enabled at $t = 5$ s, frequency and voltage are successfully restored, and reactive power is well shared. In the last scenario, the proposed controller regulates the system frequency and voltage perfectly, following load disturbances, as well as keeping active and reactive power sharing between the units. It is worth noting that the small difference between the voltage amplitude of the units is due to the measurement error.

Fig. 17 shows the impact of the information delay when regulating frequency and voltage in the experimental setup with frequent load step changes. The left column in the figure is dedicated to the frequency response, and the right column shows the voltage amplitude restoration by the DSC when the delay is 0.5 s. The delay of 20 s is examined as the worst case, and the corresponding responses are presented in Fig. 17(e) and (f). Similar to the simulation results, a time-varying delay with a standard deviation of 0.5 s was added to all of the previous cases. Overall, the experimental results show that the proposed algorithm for DSC is robust and able to maintain system stability; the increased delay only affects the settling time of the restoration process.

The experimental validation of the proposed controller when packet loss probability is set to 95% is depicted in Fig. 18; the figure shows frequency and voltage amplitude of the system during load variation. In this validation test, a 0.5-s fixed delay was introduced in order to make the experiments more realistic.

VII. Conclusion

In this paper, a distributed algorithm has been proposed for combined communication/secondary control of islanded MGs. The algorithm is based on local averaging, while each unit best an opportunity to broadcast its local value in a token ring manner. The distributed operation and the tight coupling between communication and control make the system very robust, as it removes the risk of having a single point of failure. In this wireless-communication-based algorithm, every agent calculates a new average of data in every sample time by combining the received information from other agents with its own measurements. The properties of the proposed DSC approach were evaluated at first through PHIL simulations on a four-unit paralleled autonomous MG case study. Simulation results verified that the proposed DSC method can successfully restore frequency and voltage of the system and properly equalize reactive power in the low R/X MGs even in the presence of communication delays and data packet losses. Indeed, the results showed a negligible overshoot, with slower frequency and voltage recovery to the nominal value. Finally, a small-scale experimental setup that consists of two parallel units has been assembled in the laboratory in order to confirm the validity of simulation results. It turned out that the simulation and experimental results are fairly well matched, thereby confirming the practical utility of the proposed approach.

Appendix
Broadcast Gossip Algorithms for Consensus

In its original form, the (randomized) gossip algorithm for distributed averaging operates in the following way: 1) In each iteration, a random node (i.e., agent) transmits its state variable (i.e., parameter of interest) to a random neighbor chosen from the set of neighbors within its communication range; and 2) the neighbor updates its state variable, by averaging it with the received information. If the network graph is strongly connected,[5] the algorithm converges to the consensus, and all network nodes obtain the global average of the parameter.

The broadcast gossip algorithm [21] operates in a similar way, with a main difference that the transmitting node sends its state variable to all nodes within its range; in other words, the transmissions are broadcast rather than unicast. The receiving nodes update their state variables using (19), whereas the remaining nodes maintain their state variables unchanged. Broadcast-based gossip is an asynchronous algorithm in its general version, i.e., the network nodes are not synchronized, and there is no schedule when a node will "wake up" and transmit.

Broadcast-based gossip in connected networks converges almost surely to a consensus value whose expectation is the average of initial node values, as proven in [21]. The convergence rate depends on the number of nodes, the topology of the graph, and the choice of the mixing constant β [see (19)]. Particularly, the upper bound on the convergence time (i.e., number of iterations) for broadcast-based gossip for a random geometric graph[6] is $\Omega(N^2/\log^3 N)$ [21], where N is the number of network nodes, and it is assumed that the computed estimate of the average is $1/N^{\alpha}$ close to the actual value (α is a positive constant). We note that this convergence time is shorter than the convergence time of the standard unicast gossip.

Finally, the convergence of the broadcast gossip algorithm under stochastic failures, when the broadcast transmissions are received with a probability that depends on the transmitter–receiver pair (i.e., with a nonuniform probability over receivers), is examined in [24]. It is shown that the probabilistic broadcast gossip also converges almost surely to a consensus value whose expectation is the average of initial node values.

[5] That is, there is a bidirectional path among any two nodes.

[6] A random geometric graph is typically used to model graphs of wireless networks.

References

[1] J. M. Guerrero, J. C. Vasquez, J. Matas, M. Castilla, L. G. D. Vicua, and M. Castilla, "Hierarchical control of droop-controlled AC and DC microgrids—A general approach toward standardization," *IEEE Trans. Ind. Electron.*, vol. 58, no. 1, pp. 158–172, Jan. 2011.

[2] A. Bidram and A. Davoudi, "Hierarchical structure of microgrids control system," *IEEE Trans. Smart Grid*, vol. 3, no. 4, pp. 1963–1976, Dec. 2012.

[3] C. Yuen, A. Oudalov, and A. Timbus, "The provision of frequency control reserves from multiple microgrids," *IEEE Trans. Ind. Electron.*, vol. 58, no. 1, pp. 173–183, Jan. 2011.

[4] H. S. V. S. Kumar Nunna and S. Doolla, "Multiagent-based distributed-energy-resource management for intelligent microgrids," *IEEE Trans. Ind. Electron.*, vol. 60, no. 4, pp. 1678–1687, Apr. 2013.

[5] J. M. Guerrero, P. Loh, M. Chandorkar, and T. Lee, "Advanced control architectures for intelligent microgrids—Part I: Decentralized and hierarchical control," *IEEE Trans. Ind. Electron.*, vol. 60, no. 4, pp. 1263–1270, Apr. 2013.

[6] J. Vasquez, J. M. Guerrero, M. Savaghebi, J. Eloy-Garcia, and R. Teodorescu, "Modeling, analysis, and design of stationary reference frame droop controlled parallel three-phase voltage source inverters," *IEEE Trans. Ind. Electron.*, vol. 60, no. 4, pp. 1271–1280, Apr. 2013.

[7] Q. Shafiee, J. M. Guerrero, and J. Vasquez, "Distributed secondary control for islanded microgrids—A novel approach," *IEEE Trans. Power Electron.*, vol. 29, no. 2, pp. 1018–1031, Feb. 2014.

[8] A. Bidram, A. Davoudi, F. L. Lewis, and Z. Qu, "Secondary control of microgrids based on distributed cooperative control of multi-agent systems," *IET Gener. Transm. Distrib.*, vol. 7, no. 8, pp. 822–831, Aug. 2013.

[9] F. Katiraei, R. Iravani, N. Hatziargyriou, and A. Dimeas, "Microgrids management," *IEEE Power Energy Mag.*, vol. 6, no. 3, pp. 54–65, May/Jun. 2008.

[10] A. Olshevsky and J. N. Tsitsiklis, "Convergence speed in distributed consensus and averaging," *SIAM J. Control Optim.*, vol. 48, no. 1, pp. 33–55, Feb. 2009.

[11] H. Liang, B. J. Choi, W. Zhuang, X. Shen, and A. S. Awad, "Multiagent coordination in microgrids via wireless networks," *IEEE Wireless Commun.*, vol. 19, no. 3, pp. 14–22, Jun. 2012.

[12] A. D. Dominguez-Garcia, C. N. Hadjicostis, and N. H. Vaidya, "Resilient networked control of distributed energy resources," *IEEE J. Sel. Areas Commun.*, vol. 30, no. 6, pp. 1137–1148, Jul. 2012.

[13] R. A. Gupta and M. Y. Chow, "Networked control system: Overview and research trends," *IEEE Trans. Ind. Electron.*, vol. 57, no. 7, pp. 2527–2535, Jul. 2010.

[14] K. D. Kim and P. R. Kumar, "Cyber-physical systems: A perspective at the centennial," in *Proc. IEEE*, May 13, 2012, vol. 100, pp. 1287–1308, Centennial Issue.

[15] S. K. Mazumder, M. Tahir, and K. Acharya, "Pseudo-decentralized control-communication optimization framework for microgrid: A case illustration," in *Proc. Transmiss. Distrib. Conf. Expo.*, Apr. 2008, pp. 1–8.

[16] Y. Zhang and H. Ma, "Theoretical and experimental investigation of networked control for parallel operation of inverters," *IEEE Trans. Ind. Electron.*, vol. 59, no. 4, pp. 1961–1970, Apr. 2012.

[17] D. Rua, L. F. M. Pereira, N. Gil, and J. A. P. Lopes, "Impact of multi-microgrid communication systems in islanded operation," in *Proc. IEEE PES Int. Conf. Exhib. ISGT Europe*, Dec. 5–7, 2011, pp. 1–6.
[18] S. Boyd, A. Ghosh, B. Prabhakar, and D. Shah, "Randomized gossip algorithms," *IEEE Trans. Info. Theory*, vol. 52, no. 6, pp. 2508–2530, Jun. 2006.
[19] J. M. Guerrero, L. Garcia de Vicuna, J. Matas, M. Castilla, and J. Miret, "Output impedance design of parallel-connected UPS inverters with wireless load-sharing control," *IEEE Trans. Ind. Electron.*, vol. 52, no. 4, pp. 1126–1135, Aug. 2005.
[20] C. K. Sao and P. W. Lehn, "Autonomous load sharing of voltage source converters," *IEEE Trans. Power Del.*, vol. 20, no. 2, pp. 1009–1016, Apr. 2005.
[21] T. C. Aysal, M. E. Yildiz, A. D. Sarwate, and A. Scaglione, "Broadcast gossip algorithms for consensus," *IEEE Trans. Signal Process.*, vol. 57, no. 7, pp. 2748–2761, Jul. 2009.
[22] *Token Ring Access Method and Physical Layer Specification*, IEEE 802.5-1998, 1998.
[23] D. Shah, "Gossip Algorithms," *Foundations Trends Netw.*, vol. 3, no. 1, pp. 1–125, Jun. 2009.
[24] T. C. Aysal, A. D. Sarwate, and A. G. Dimakis, "Reaching consensus in wireless networks with probabilistic broadcast," in *Proc. Allerton Conf. Commun., Control Comput.*, Monticello, IL, USA, Sep. 2009, pp. 732–739.

Qobad Shafiee (S'13) received the M.S. degree in electrical engineering from Iran University of Science and Technology (IUST), Tehran, Iran, in 2007. He is currently working toward the Ph.D. degree in the Department of Energy Technology, Aalborg University, Aalborg, Denmark.

He was with the Department of Electrical and Computer Engineering, University of Kurdistan, Sanandaj, Iran, from 2007 to 2011. His main research interests include hierarchical control, networked control systems, and power quality in microgrids.

Čedomir Stefanović (S'05–M'11) received the Dipl.-Ing., Mr.-Ing., and Ph.D. degrees in electrical engineering from the University of Novi Sad, Novi Sad, Serbia.

Since 2004, he has been with the Department of Power, Electronics and Communication Engineering, University of Novi Sad, where he is currently an Assistant Professor. He is currently a Postdoctoral Researcher with the Department of Electronic Systems, Aalborg University, Aalborg, Denmark. His research interests include communication theory, including design and analysis of enhanced random-access mechanisms, distributed algorithms for wireless ad hoc and sensor networks, and frame synchronization.

Tomislav Dragičević (S'09) received the M.E.E. and Ph.D. degrees from the University of Zagreb, Zagreb, Croatia, in 2009 and 2013, respectively.

Since 2010, he has been actively cooperating in an industrial project related with the design of electrical power supply for remote telecommunication stations. He is currently a full-time Postdoctoral Researcher with Aalborg University, Aalborg, Denmark. His fields of interest include modeling, control, and energy management of distributed power systems based on renewable sources and energy storage technologies.

Petar Popovski (S'97–A'98–M'04–SM'10) received the Dipl.-Ing. degree in electrical engineering and the Magister Ing. degree in communication engineering from Saints Cyril and Methodius University of Skopje, Skopje, Macedonia, in 1997 and 2000, respectively, and the Ph.D. degree from Aalborg University, Aalborg, Denmark, in 2004.

He is currently a Professor with Aalborg University. He has more than 160 publications in journals, conference proceedings, and books and has more than 25 patents and patent applications. His research interests include wireless communication and networking, information theory, and protocol design.

Dr. Popovski has received the Young Elite Researcher Award and the SAPERE AUDE Career Grant from the Danish Council for Independent Research. He has received six best paper awards, including three from the IEEE. He serves on the editorial board of several journals, including the IEEE COMMUNICATIONS LETTERS (Senior Editor), the IEEE JSAC COGNITIVE RADIO SERIES, and the IEEE TRANSACTIONS ON COMMUNICATIONS. He is a Steering Committee Member for the IEEE INTERNET OF THINGS JOURNAL and the Chair of the IEEE Communications Society subcommittee on Smart Grid Communications.

Juan C. Vasquez (M'12) received the B.S. degree in electronics engineering from Autonomous University of Manizales, Manizales, Colombia, in 2004 and the Ph.D. degree from the Technical University of Catalonia, Barcelona, Spain, in 2009.

He taught courses on digital circuits, servo systems, and flexible manufacturing systems at Autonomous University of Manizales. He was also a Postdoctoral Assistant and taught courses on renewable energy systems with the Department of Automatic Control Systems and Computer Engineering, Technical University of Catalonia. Since 2011, he has been an Assistant Professor of microgrids with the Department of Energy Technology, Aalborg University, Aalborg, Denmark, where he is coresponsible for the microgrids research program. His current research interests include operation, power management, hierarchical control, and optimization applied to distributed generation in ac/dc microgrids.

Josep M. Guerrero (S'01–M'04–SM'08) received the B.S. degree in telecommunications engineering, the M.S. degree in electronics engineering, and the Ph.D. degree in power electronics from the Technical University of Catalonia, Barcelona, Spain, in 1997, 2000, and 2003, respectively.

He was an Associate Professor with the Department of Automatic Control Systems and Computer Engineering, Technical University of Catalonia, teaching courses on digital signal processing, field-programmable gate arrays, microprocessors, and control of renewable energy. Since 2011, he has been a Full Professor with the Department of Energy Technology, Aalborg University, Aalborg, Denmark, where he is responsible for the microgrid research program. His research interests include power electronics converters for distributed generation and distributed energy storage systems, control and management of microgrids and islanded minigrids, and photovoltaic and wind power plants control.